

Planet formation and long-term stability in a very eccentric stellar binary

Jakob Stegmann¹, Evgeni Grishin^{2,3}, Cole Johnston^{4,1,5},
Nora L. Eisner^{6,7}, Stephen Justham¹, Selma E. de Mink^{1,8},
Hagai B. Perets^{9,10}

¹Max Planck Institute for Astrophysics, Karl-Schwarzschild-Str. 1,
85748 Garching, Germany.

²School of Physics and Astronomy, Monash University, Clayton, VIC
3800, Australia.

³OzGrav: Australian Research Council Centre of Excellence for
Gravitational Wave Discovery, Clayton, VIC 3800, Australia.

⁴Department of Physics, University of Surrey, Guildford, Surrey, GU2
7XH, UK.

⁵Institute of Astronomy, KU Leuven, Celestijnenlaan 200D, 3001
Leuven, Belgium.

⁶Center for Computational Astrophysics, Flatiron Institute, 162 Fifth
Avenue, New York City, NY 10010, USA.

⁷Department of Astrophysical Sciences, Princeton University, Princeton,
NJ 08544, USA.

⁸Ludwig-Maximilians-Universität München, Geschwister-Scholl-Platz 1,
80539 München, Germany.

⁹Physics Department, Technion - Israel Institute of Technology, 3200003
Haifa, Israel.

¹⁰Astrophysics Research Center of the Open University (ARCO),
4353701 Raanana, Israel.

Contributing authors: jstegmann@mpa-garching.mpg.de;

Abstract

Planets orbiting one of the two stars in a binary are vulnerable to gravitational perturbations from the other star. Particularly, highly eccentric companion stars risk disrupting planetary orbits, such as in the extreme system TOI 4633 where

close encounters between the companion and a gas giant planet in the habitable zone make it one of the most fragile systems discovered so far. Here, we report that TOI 4633’s planet likely survived these encounters throughout the system’s age by orbiting retrograde relative to the binary, stabilised by the Coriolis force. Using direct N -body simulations, we show it otherwise tends to collide with the binary stars or becomes free-floating after getting ejected. A retrograde planetary orbit has profound implications for TOI 4633’s formation and evolution, suggesting an extraordinary history where its eccentric companion was likely randomly captured after planet formation in a single-star system. Alternatively, if stars and planet are born in situ from the same gas clump, we show the planet must have formed at sub-snow-line distances, contrary to the conventional core-accretion model. Our study highlights the importance of considering the long-term stability (\gtrsim Gyr) of planets in eccentric binaries and demonstrates that the mere existence in such dynamically hostile environments places strong constraints on their orbital configuration and formation.

TOI 4633 is a remarkable system that was recently discovered as part of the Citizen Science Project Planet Hunters TESS [1]. It consists of two solar-like stars moving around one another on a highly eccentric orbit ($e_B = 0.91 \pm 0.03$) and a transiting mini-Neptune (TOI 4633c) in the habitable zone around one of the stars (TOI 4633A). The large eccentricity causes the stellar binary companion (TOI 4633B) to closely encounter the planet at a periapsis $r_{p,B} \approx 4.4$ AU (see sketch in Figure 1), once every binary period of about 230 yr. Of more than two hundred planets discovered in stellar binaries, these close encounters make TOI 4633c one of the most dynamically fragile planets known to date.

It is confounding how such a planet could have formed and survived throughout TOI 4633’s age of $t_{\text{age}} = 1.3 \pm 0.3$ Gyr [1]. The periodic gravitational perturbation from the closely encountering stellar companion should pose a significant risk to the stability of TOI 4633c’s orbit, potentially resulting in its ejection from the system or a collision with the host star. Indeed, previous stability criteria which were inferred from a grid of direct three-body integrations of single s-type¹ planets in binary systems suggest that TOI 4633c is on the verge of destruction. Figure 2 shows that TOI 4633c’s semi-major axis $a_{\text{Ac}} = 0.847 \pm 0.061$ AU exceeds the widely used critical threshold a_{crit} of dynamical stability from Holman and Wiegert [2]. While their grid-based interpolation for stability is formally inapplicable to TOI 4633c since they only consider co-planar orbits with eccentricities up to $e_B \leq 0.8$, Eisner et al. [1] conducted simulations to specifically recover dynamically stable configurations of TOI 4633. As a result, the planet could only be stable if the mutual inclination angle i_{tot} between its orbit around TOI 4633A and the orbital plane of the stellar binary TOI 4633AB is between $0^\circ \lesssim i_{\text{tot}} \lesssim 40^\circ$ (prograde) or $140^\circ \lesssim i_{\text{tot}} \lesssim 180^\circ$ (retrograde), whereas highly inclined orbits ($40^\circ \lesssim i_{\text{tot}} \lesssim 140^\circ$) become quickly unstable (see Figure 1 for a schematic overview). The fragility of TOI 4633 is even more concerning given the common expectation that planets of that mass ($m_c \approx 50 M_\oplus$, see Supplementary Table 1 for a list of all

¹S-type (circumstellar) planets such as TOI 4633c orbit either one of the two stars of a binary (see Fig. 1), whereas p-type (circumbinary) planets orbit the binary as a whole at a much larger distance.

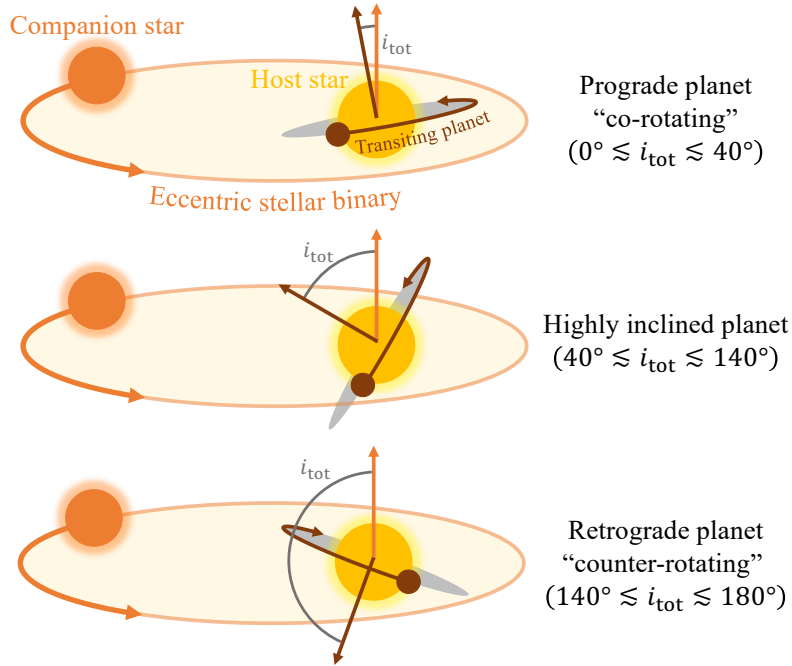


Fig. 1 Schematic overview of the eccentric binary system TOI 4633 hosting an s-type planet in the habitable zone. The planet was discovered via the transit detection method which leaves the spatial orientation of its orbit unknown. It may either be (a) prograde, i.e., the planet and the companion star share the same sense of rotation, (b) highly inclined, or (c) retrograde as illustrated in the three panels. We find the planet likely to orbit retrograde in order to survive the periodic gravitational perturbations throughout the system’s lifetime of $t_{\text{age}} = 1.3 \pm 0.3$ Gyr.

parameters) need to form beyond the snow line at $a_{\text{Ac}} \gtrsim 3.0$ AU [3, 4] where the temperature is low enough for volatile compounds like water to condense into solid ice grains. Beyond the snow line the detrimental effect of the encountering companion would be even stronger, or it may truncate the protostellar disc around the host star preventing the planet to form.

Previous pioneering studies to assess the stability of general or specific s-type planets largely rely on direct N -body simulations that only cover several to tens of Myr [1, 2, 6–17]. This is only a small fraction $\lesssim 1\%$ of the estimated age $t_{\text{age}} \gtrsim$ Gyr of the stars in TOI 4633 and other typical low-mass stellar hosts of observed planets. Simulating systems like TOI 4633, which are on the verge of destruction, up to a maximum integration time $t_{\text{max}} \ll t_{\text{age}}$ could yield false positive stable solutions. The perturbation from the stellar companion could accumulate to destabilise the planet between t_{max} and t_{age} . Here, we present a suite of direct N -body simulations [18] of TOI 4633 which were conducted for a maximum integration time $t_{\text{max}} = t_{\text{age}}$ to evolve different realisations of TOI 4633 (see Methods) which are consistent with the observed parameters (Supplementary Table 1). As a default, TOI 4633 is arranged as a 2+1 triple

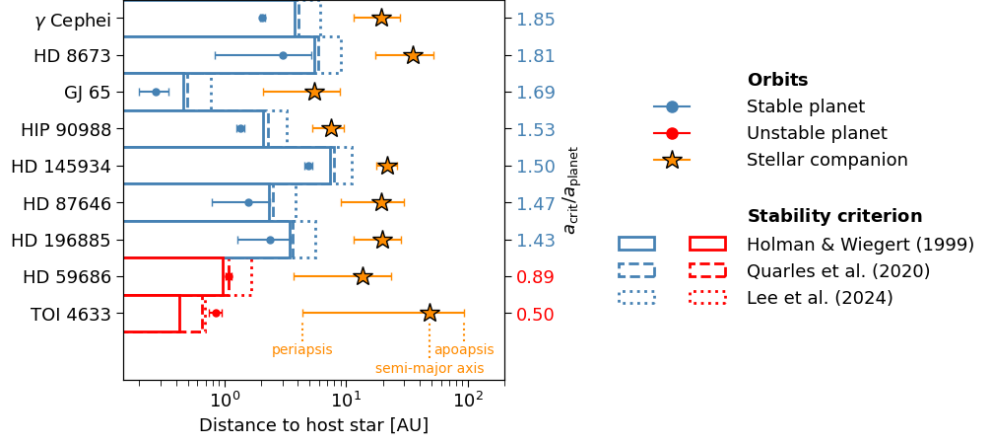


Fig. 2 Orbital hierarchy of previously discovered stellar binaries with s-type planets that are close to being dynamically unstable. We show all systems with $a_{\text{crit}}/a_{\text{planet}} < 2$ with the semi-major axis of the (outermost) planet a_{planet} [2] contained in The Extrasolar Planets Encyclopaedia [5] and sort them according to their presumed stability by $a_{\text{crit}}/a_{\text{planet}}$. Orange star symbols indicate the semi-major axis a_{B} of the stellar binary while horizontal lines extend from its periapsis $r_{p,B} = a_{\text{B}}(1 - e_{\text{B}})$ to apoapsis $r_{a,B} = a_{\text{B}}(1 + e_{\text{B}})$. Similarly, blue and red circles and lines indicate the semi-major axis, periapsis, and apoapsis of the planet, respectively. Blue and red bars extend to the critical semi-major axis a_{crit} for the planetary orbit above which it would not be dynamically stable according to Holman and Wiegert [2] (solid), Quarles et al. [6] (dashed), and Lee et al. [7] (dotted). For the criterion of Holman and Wiegert [2], we show if a planet is stable (blue) or not (red) and indicate the numerical value on the right.

composed of the two stars TOI4633A and B, as well as the planet TOI4633c orbiting star A (Figure 1) and explore plausible variants below. The planet TOI4633c was discovered via the transit detection method, i.e., by causing dips in stellar brightness when it passes in front of its host stars and blocks some of its light. As illustrated in Figure 1, the dip in stellar brightness does not reveal at which angle of incidence the planet moves in front of the star, which effectively leaves the mutual inclination i_{tot} between the planet orbit and the binary plane the only fundamentally unconstrained parameter of TOI4633 (see Methods). Therefore, we initialise the simulations of TOI4633 by choosing different values of i_{tot} between 0° and 180° (see Methods). All simulations are terminated if either the planet survives by reaching the maximum integration time $t_{\text{max}} = t_{\text{age}}$ or if the planet becomes unstable due to a collision with a star or by getting ejected from the system.

Figure 3 presents example systems that illustrate the three qualitatively different evolutionary outcomes by showing the trajectories of the stars and the planet and their relative separations as a function of time. In the first two examples (panels a – c and d – f) the planets start out on prograde orbits ($i_{\text{tot}} < 40^\circ$). In these cases, the periodic forcing from the stellar companion at periapsis impulsively induces a chaotic evolution of the planets around their host which eventually leads to a collision and ejection, respectively. Notably, the planet in the second example (panels d – f) does get ejected and becomes a free-floating planet [19] after it had been captured

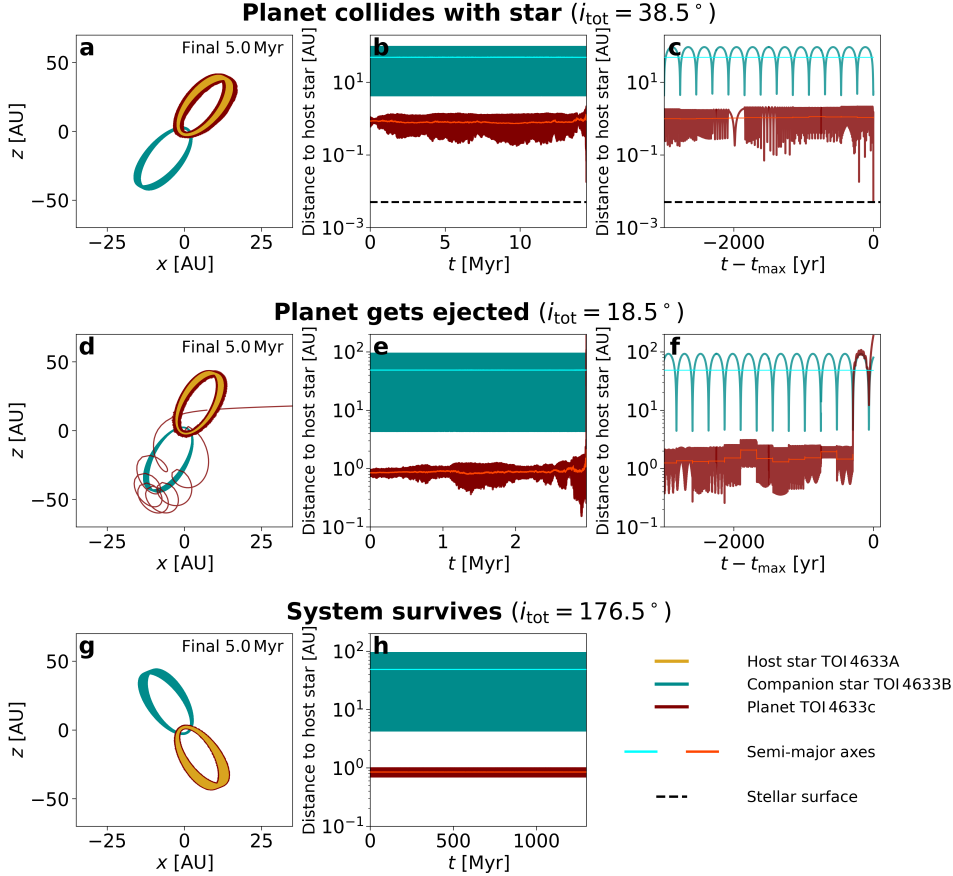


Fig. 3 Three examples for the evolution of TOI 4633 in a 2+1 configuration. The system in the upper row (panels a – c) starts from a mutual inclination $i_{\text{tot}} = 38.5^\circ$ leading to a collision of planet TOI4633c with its host star TOI4633A after $t_{\text{max}} \approx 1.4 \times 10^7$ yr. The system in the middle row (d – f) starts from a mutual inclination $i_{\text{tot}} = 18.5^\circ$ resulting in the ejection of the planet after $t_{\text{max}} \approx 3.0 \times 10^6$ yr. Only in the lower row (g and h) does the system remain intact throughout its estimated age $t_{\text{max}} = t_{\text{age}} = 1.3 \times 10^9$ yr after starting from $i_{\text{tot}} = 176.5^\circ$. The leftmost panels (a, d, and g) display the projected trajectories in the centre-of-mass frame of the two stars (purple and red) and the planet (cyan) during the final 5.0×10^6 yr. The middle panels (b, e, and h) show the relative separations of the companion star TOI4633B and the planet with respect to the host star as a function of time. Light colours indicate the semi-major axes of their orbits around the host and the dashed line corresponds to the combined radius $r_A + r_{Ac}$ of the host star and the planet. For the non-surviving systems, the rightmost panels (c and f) contain a zoom-in of the last 3×10^3 yr before the planetary collision and ejection, respectively.

by the stellar companion and followed its motion for one orbit. We find this “star hopping” [20] to be a common event preceding a planetary ejection. The planet in the third example (panels g and h) is initialised on a retrograde orbit ($i_{\text{tot}} > 140^\circ$). It remains largely unaffected by the stellar companion and survives the entire evolution for $t_{\text{max}} = t_{\text{age}}$. Meanwhile, in all three examples the stellar binary remains largely unaffected by the presence of the planet except that it causes a notable precession of

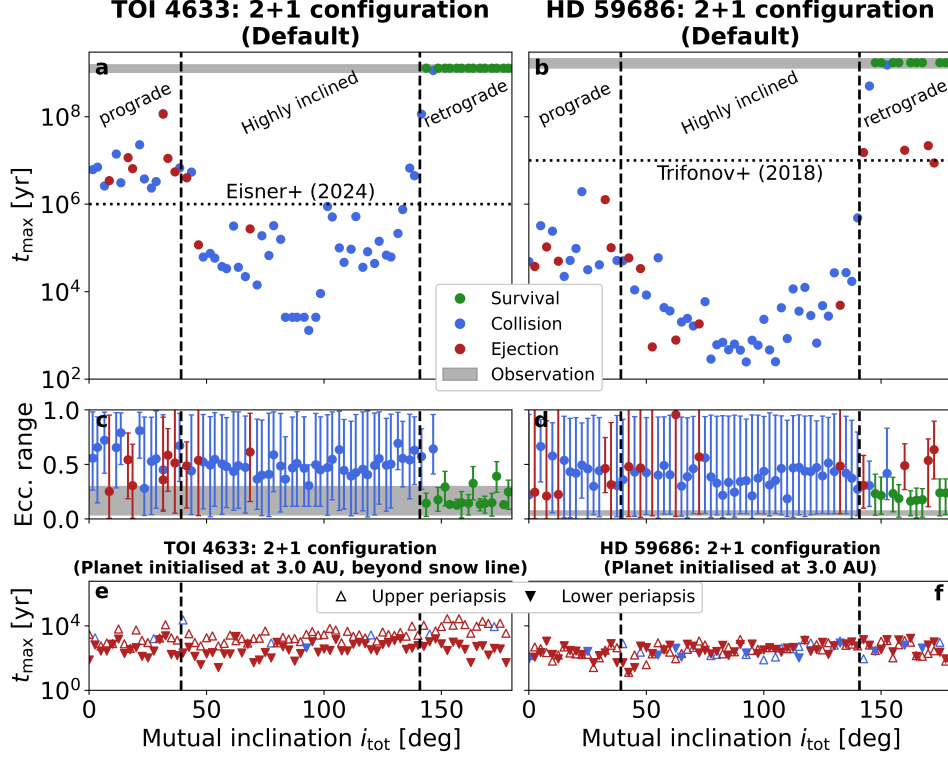


Fig. 4 Evolutionary outcomes of the simulations as a function of the mutual inclination i_{tot} between the planetary and stellar orbits. Green markers indicate successful integrations until the maximum integration time $t_{\text{max}} = t_{\text{age}}$, blue markers indicate planetary collisions with either one of the stars prior to t_{age} , and maroon markers indicate ejections of the planet. The left column shows TOI 4633 in our default 2+1 configuration where planet b is ignored. The right column shows HD 59686. The upper row (panels a and b) displays the maximum integration time until a certain evolutionary outcome is met. The middle row (panels c and d) indicates the range of orbital eccentricity (minimum, mean, and maximum) the planet attains throughout its evolution. In the lower row (panels e and f) the planet is initialised on a circular orbit at a semi-major axis of 3.0 AU (corresponding to the snow line for TOI 4633 [3, 4]) and, within their one-sigma uncertainty, the binary semi-major axis a_B and eccentricity e_B are chosen to give the maximum (unfilled triangles) and minimum periapsis $r_{p,B} = a_B(1 - e_B)$ (filled triangles). Vertical dashed lines indicate the Kozai angles $i_{\text{tot}} = 39.2^\circ$ and 140.77° . Horizontal dotted lines show the maximum integration time assumed by Eisner et al. [1] and Trifonov et al. [16] to simulate TOI 4633 and HD 59686, respectively. Grey-shaded areas indicate the observational constraints on the age and the present-day orbital eccentricity of TOI 4633 and HD 59686, respectively.

the binary periapsis by a few degrees (left panels a, d, and g), which is consistent with a precession timescale of $T_{\text{prec},B} \approx 170$ Myr (see Methods).

Figure 4, panel a, shows all simulation outcomes (survival in green, collision in blue, and ejection in red) as a function of the mutual inclination i_{tot} between the orbit of the planet and the stellar binary. The stability of a three-body system is dependent on the mutual inclination between the inner and outer system, where retrograde orbits are known to be more stable than prograde ones. This was first shown by [21],

and arises from Coriolis effect [22], as we discuss below. Another dependence arises from secular von Zeipel-Lidov-Kozai [vZLK; 23–25] effect, which can excite the eccentricities of the inner binary, making the system less stable, in particular between the so-called Kozai angles $40^\circ \lesssim i_{\text{tot}} \lesssim 140^\circ$ [26, 27]. Due to these effects, the simulations exhibit three characteristic regimes. Between the Kozai angles the stellar companion exerts a torque causing large-amplitude eccentricity oscillations of the planetary orbit through vZLK effect, which most often leads to a collision with the host star or ejection from the system. The vZLK effect is suppressed for less inclined orbits at $i_{\text{tot}} \lesssim 40^\circ$ (prograde) and $i_{\text{tot}} \gtrsim 140^\circ$ (retrograde), in which case the planet survives for longer times. However, a striking asymmetry unravels for longer integration times where the large majority of retrograde simulations survives throughout the entire simulated age of TOI 4633, whereas all prograde planets either collide with the star or get ejected beforehand. Notably for the case of prograde orbits, dynamical instabilities occur significantly later than $t_{\text{max}} = 1 \text{ Myr}$. This effectively renders the standard stability assessment based on shorter integration times inapplicable to determine the stability of systems like TOI 4633 [e.g., 1, 2]. A retrograde planetary orbit is further supported by its eccentricity evolution displayed in panel c, which includes its minimum, maximum, and mean eccentricity throughout the integration. Only in the retrograde case do we find it to be largely consistent with its observed value $e_{\text{Ac}} = 0.117^{+0.186}_{-0.085}$. The different stability of near-coplanar prograde and retrograde orbits in hierarchical three-body systems is a well-known phenomenon, which is clearly visible in the case of TOI 4633. This is because, in the frame rotating with the motion of the stellar binary, the planet experiences a Coriolis force [22]. The force’s direction depends on the relative sense of rotation between binary orbit and planet orbit. Thus, it pushes the planet further away from its host in the co-rotating, prograde case, whereas pushing it closer in the counter-rotating, retrograde case, i.e., making the planet orbit around the host less or more stable, respectively [22].

TOI 4633 contains a second planet (TOI 4633b) that was discovered through radial velocity variations to move around either of the stars at a much tighter orbit than TOI 4633c [1]. We have tested various configurations including TOI 4633b whose orbital properties are poorly constrained from observations, which we show in Supplementary Figure 1. First, we arrange TOI 4633 as a 3+1 quadruple with planet b orbiting star A, where we closely align the orbits of both planets but ensure that planet b is not seen as a transit (panels a and c), align it with the stellar binary TOI 4633AB (panels b and d), and randomly orient planet b’s orbit (panels e and g). Second, we consider a 2+2 quadruple with planet b orbiting star B, where we align its orbit with that of the stellar binary TOI 4633AB (panels f and h) and draw a random orientation (panels i and k). In all cases, we keep varying the orbital orientation of planet c (see Methods). In these cases, we generally observe a larger scatter in the evolutionary outcomes so that some retrograde configurations do not survive, mostly because of planet b becoming unstable. Nevertheless, all studied cases result in similar retrograde-only stable configurations and we conclude that regardless of the orbital configuration of planet b, the quadruple TOI 4633 could only survive until $t_{\text{max}} = t_{\text{age}}$ if planet c’s orbit is retrograde with respect to the stellar binary.

These findings relax if we assume the largest periapsis of the stellar binary allowed by the observational one-sigma uncertainties on its eccentricity $e_B = 0.91 \pm 0.03$ and semi-major axis $a_B = 48.6_{-3.5}^{+4.4}$ AU. In Supplementary Figure 1, panels j and l, we show our default 2+1 configuration initialised with $e_B = 0.88$ and $a_B = 53.0$ AU, i.e., $r_{p,B} = a_B(1 - e_B) \approx 7.5a_{Ac}$. In this case, also all prograde planets ($0^\circ \lesssim i_{tot} \lesssim 40^\circ$) and even a few highly inclined systems within the Kozai angles ($40^\circ \lesssim i_{tot} \lesssim 140^\circ$) would survive. In order to further test the stability of prograde orbits within the observational uncertainty, we consider the prograde and co-planar configuration ($i_{tot} = 0.0^\circ$) and systematically vary the binary eccentricity and semi-major axis within the one-sigma uncertainty. As shown in Supplementary Figure 2 the prograde planet orbit would still get destabilised for most of the allowed parameter space and survives only if the binary periapsis is $r_{p,B} \gtrsim 5.9a_{Ac} \approx 5.0$ AU. Following the Bayesian parameter estimation of Eisner et al. [1] to construct posterior distributions for a_B and e_B from the observations of TOI 4633 (see contours in Supplementary Figure 2), we find an 80.0% probability that $r_{p,B}$ is below the threshold of 5.0 AU, where only retrograde planetary orbits are found to be stable. Thus, it is likely that the binary periapsis is indeed small enough to prevent any stable prograde configurations of the planet, though a wider companion allowing other configurations cannot be ruled out. Regardless, either scenario – a sufficiently close companion ($r_{p,B} \lesssim 5.0$ AU) which enforces a retrograde planetary orbit, or a wider companion ($r_{p,B} \gtrsim 5.0$ AU) that also allows prograde planetary orbits – challenges our understanding of planet formation, as explained in the following.

We conducted additional simulations of TOI 4633 in the 2+1 configuration where we initialised the planet on a circular orbit beyond the snow line at $a_{Ac} = 3.0$ AU [3, 4]. Figure 4, panel e, shows that the planet rapidly destabilises mostly through ejections in less than about 10^4 yr. These findings are nearly independent of the mutual inclination and even hold if we assume the observational upper bound on the binary periapsis (unfilled triangle markers). This timescale is much shorter than the planet could radially migrate inwards to its current orbit [28]. Therefore, the planet could not have formed beyond the snow line in a circumprimary protostellar disc alongside an existing binary companion but would need to form much closer to its host, perhaps near its current position. Such in-situ formation at sub-snow-line distances is not expected in the standard core-accretion model [29–31]. Moreover, close binary companions with projected separations $\rho < 50$ AU significantly reduce both the occurrence rate and longevity of protoplanetary discs [32] and diminish exoplanet occurrence rates [33]. Additionally, a large binary eccentricity would further shorten the disc’s lifetime and spatial extent, making planet formation in such systems feasible only with a massive, low-eccentricity, self-gravitating disc, which is improbable [34, 35]. Alternatively, the stellar companion might have been captured as a result of stellar scattering in a dense environment, after the planet has formed. However, recent star-formation simulations [36] show that although $\sim 20\%$ of stars experienced an exchange interaction already during the star-formation, these mostly originated from disintegration of higher multiplicity systems, and not from single-formed stars which became binaries. Nevertheless, later exchanges in the cluster environment could occur on longer timescales. This seems plausible for three reasons: i) In the absence of a perturbing stellar companion,

the planet could have formed beyond the snow line and subsequently migrated to its current position. ii) The large eccentricity is a probable result of dynamical assembly of the binary [37–39]. iii) If the planet orbit is indeed retrograde relative to the binary it would be a possible outcome of a star captured from a random direction [38]. Conversely, if the star and planet had formed from the same gas clump, their orbital angular momenta would align, making a prograde orientation much more plausible. Other proposed mechanisms to form retrograde planets from long-term interactions with another more distant planet [40] or from planet-planet scatterings among p-type (circumbinary) planets [41] seem implausible to explain TOI 4633c’s orbit. Another outer planet would have even less likely survived the presence of the binary companion, while Ref. [41] showed that the formation of retrograde s-type planets from p-type planet scatterings is suppressed for large binary eccentricities.

From the confirmed sample of discovered exoplanets, only HD 59686 [42] shares similar properties of a highly eccentric stellar binary ($a_B \approx 13.6$ AU, $e_B \approx 0.73$) and dynamical fragility ($a_{Ab} \approx 1.1$ AU, cf. Figure 2). Trifonov et al. [16] conducted numerical integrations of HD 59686 for up to $t_{\max} = 10$ Myr (not considering the possibility for planet-star collisions), finding it stable for retrograde orbits with $145^\circ \lesssim i_{\text{tot}} \lesssim 180^\circ$ and in a narrow region of prograde solutions locked in a secular apsidal alignment. However, unlike in TOI 4633, the planet and stellar companion in HD 59686 were discovered through radial-velocity measurements which leave the orbital orientation of the binary and planet less constrained (Supplementary Table 1) greatly increasing the allowed parameter space and making its stability analysis less complete. We conducted our analysis for HD 59686 up to its estimated age $t_{\text{age}} = 1.73 \pm 0.47$ Gyr [42] (see Methods), and find qualitatively similar results as in TOI 4633. The right column of Figure 4 shows that we only find retrograde solutions to be stable (albeit there is less agreement with the observed eccentricity range in panel d), that the planet would rapidly disperse if it was placed further outside towards HD 59686’s snow line (~ 9.7 AU [42]), and Supplementary Figure 3 shows no stable prograde solution within the observational uncertainty of the semi-major axis and orbital eccentricity of the stellar binary. While the same formation scenarios like above may also explain the origin of the planet in the hostile binary HD 59686AB, Ortiz et al. [42] highlight another plausible alternative. Unlike in TOI 4633, the binary is composed of evolved stars, with the companion likely being a white dwarf. Its progenitor star must have initiated a mass-transfer episode onto HD 59686A. This would have led to an accretion disk around it from which the planet may have formed as a second-generation circumstellar planet [43, 44], alleviating the need for long-term stability over t_{age} . While the details of this scenario are uncertain, we summarise that TOI 4633 harbours the only known planet whose origin could be either explained by sub-snow-line in-situ formation or late dynamical assembly of the binary companion.

Our analysis of TOI 4633 could serve as a blueprint to study the orbits of many transiting s-type planets which are soon detectable with the spacecraft *Plato* and whose hosts could also reveal a fully astrometrically resolvable companion in the coming data release of *Gaia* (DR4). After its launch in late 2026, *Plato* is designed to detect about ~ 4600 planets transiting stellar hosts with V -band magnitudes $V \leq 13$ at periods $T \lesssim 10^3$ days [45]. We find that in the latest *Gaia* data release (DR3) a

fraction of 4.0 percent of all bright stars ($G \leq 13$) in the field-of-view of the first *Plato* Long-duration Observation Phase (LOPS2) have stellar companions on astrometrically resolved orbits with $T_B \lesssim 10^3$ days. This fraction might increase in *Gaia* DR4 (after mid-2026), potentially up to the close binary fraction of 10 – 20 percent observed for low-mass stars [46]. Unless a close stellar binary companion strongly suppresses the presence of planets, we can therefore plausibly expect tens to a few hundred discoveries of s-type planets in close binary stars, where, like in TOI 4633, *Plato* transits and *Gaia* astrometry only leave i_{tot} fundamentally unconstrained. This presents an opportunity to test the retrograde orbit hypothesis via radial velocity observations and the Rossiter-McLaughlin effect [47–49] for potentially hundreds of systems discovered by *Plato*. As demonstrated in this work, our method could serve as a blueprint to uncover their orbital state and to constrain their evolutionary past.

Methods

We use the direct N -body code *Rebound* [18] to simulate different orbital configurations of TOI 4633 using the built-in Gragg-Bulirsch-Stoer integrator [50, 51] with relative and absolute tolerances of 10^{-12} . We have also tested evolving several systems (including the long-integration survivors) with the more accurate (albeit computationally more expensive) Integrator with Adaptive Step-size control at 15th order (IAS15) [52, 53] without finding a difference in the evolutionary outcome. In order to initialise our default 2+1 configuration (Figure 4, panel a and c), we adopt all observed mean values reported in Supplementary Table 1 for the masses m_A , m_B , and m_c , semi-major axes a_B and a_{Ac} , orbital eccentricities e_B and e_{Ac} , as well as orbital angles in the observer frame ω_B (binary’s argument of pericentre), Ω_B (binary’s longitude of ascending node), i_B (binary’s inclination relative to the line of sight), and i_{Ac} (planet’s inclination relative to the line of sight). In each simulation we set the observationally unconstrained longitude of the ascending node of the planet to $\Omega_{Ac} = 0^\circ, 5^\circ, \dots, 355^\circ$ (summing up to 72 simulations in total), resulting in a different mutual inclination i_{tot} as

$$\cos i_{\text{tot}} = \cos i_B \cos i_{Ac} + \sin i_B \sin i_{Ac} \cos(\Omega_B - \Omega_{Ac}). \quad (1)$$

Since the large measurement uncertainties of the planet’s argument of pericentre ω_{Ac} make it effectively unconstrained too, we opt to sample it randomly between 0 and 360° in each simulation. Furthermore, we pick random initial phases in time by sampling the mean anomalies of the stellar and planetary orbits from a uniform distribution between 0 and 360° . Each simulation is terminated after it reaches a maximum integration time $t_{\text{max}} = 1.3 \text{ Gyr}$, if the distance between TOI 4633A and TOI 4633c exceeds 100 AU, or if the distance between TOI 4633c to either of the stars gets smaller than their combined radii $r_A + r_c$ and $r_B + r_c$, respectively, which are adopted from the observations (Supplementary Table 1). In order to justify our limit of 100 AU, we repeat the simulation of several ejected systems and verified that they indeed reach a much larger distance of 10^3 AU .

Furthermore, we conduct simulations in which we take the presence of planet TOI 4633b into account. For those, we initialise 72 simulations exactly like above and add planet b as follows. In the first configuration, we put it on an orbit around the

host star A with $i_{Ab} = 88.0^\circ$ and $\Omega_{Ab} = \Omega_{Ac}$ (Figure 1, panels a and c). This 3+1 configuration is adopted from Eisner et al. [1] and represents a near-alignment with the orbit of c where the slight difference in inclination is to ensure that planet b is not observed as a transit. Second, we align its orbit with the stellar binary, i.e., $i_{Ab} = i_B$ and $\Omega_{Ab} = \Omega_B$ (panels b and d). Third, we keep this 3+1 configuration but randomise the spatial orientation of the orbit of planet b, i.e., we draw Ω_{Ab} , ω_{Ab} , and $\cos i_{Ab}$ from uniform distributions (panel e and g). The set-up of the latter two configurations is repeated but with planet b orbiting the other star TOI 4633B (panels f and h and panels e and g, respectively). In each of the configurations we randomise the mean anomaly and ω_{Ab} of the planet, calculate its mass as $m_b \times \sin i_{Ab} = 106.8 M_\oplus$, and compute its semi-major axis from Kepler’s Third law

$$a_{Ab} = \sqrt[3]{\frac{Gm_{\text{tot}}T_{Ab}^2}{4\pi^2}}, \quad (2)$$

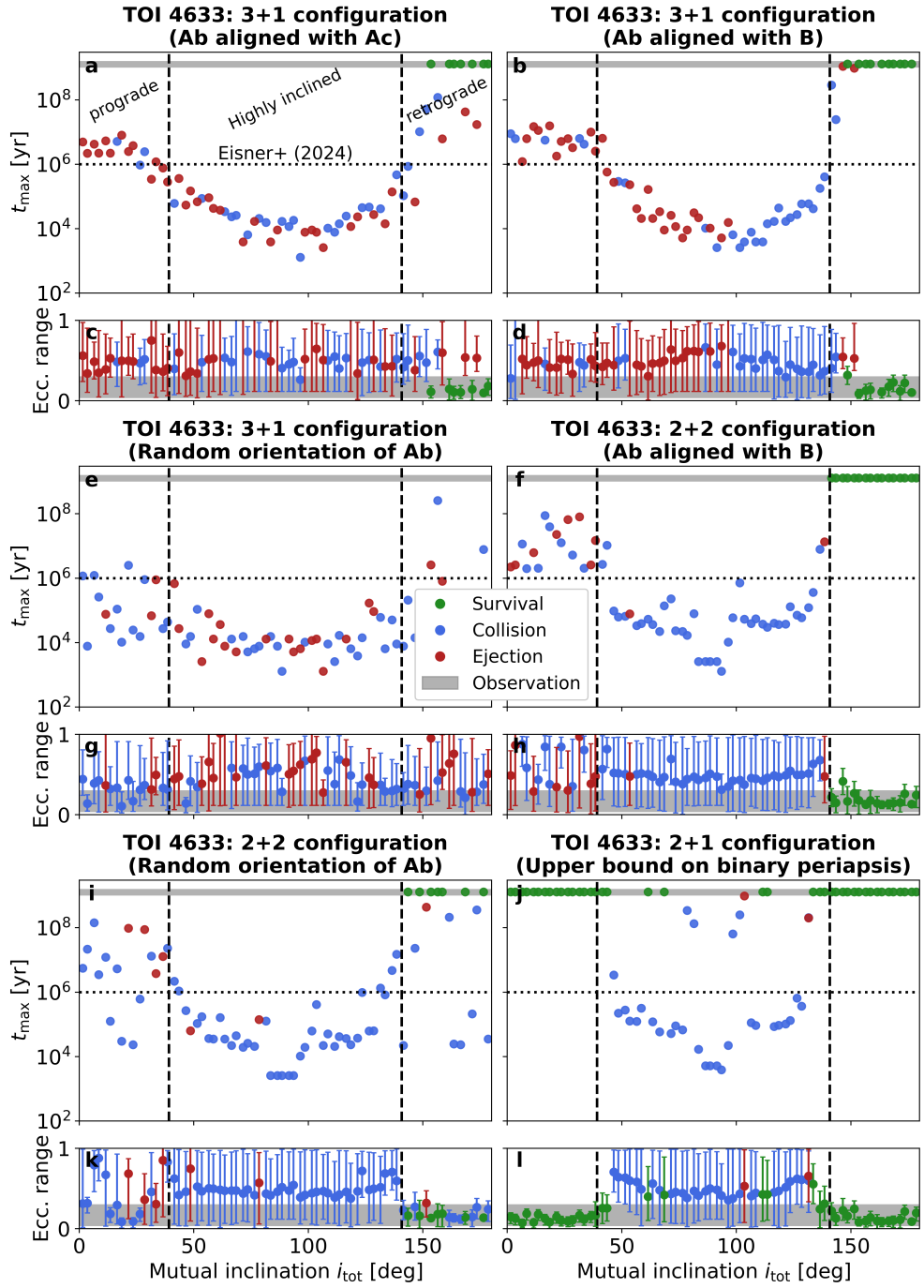
where G is the gravitational constant and the total mass is $m_{\text{tot}} = m_A + m_b$ for the 3+1 configurations and $m_{\text{tot}} = m_B + m_b$ for the 2+2 configurations. In all of these quadruple simulations, we also terminate the integration if planet b gets ejected or collides with one of the stars. Lacking a radius estimate for the planet we assume $r_b = 10 R_\oplus$ which is typical for planets of that mass [54].

Moreover, we explored auxiliary 2+1 configurations of TOI 4633 with different values for the binary semi-major axis and eccentricity within the observational one-sigma uncertainty $a_B = 48.6_{-3.5}^{+4.4}$ AU and $e_B = 0.91 \pm 0.03$, respectively. Firstly, we have initialised the largest binary periapsis, i.e., $a_B = 53.0$ AU and $e_B = 0.88$ and choose the other parameters as described above (panels j and l). Secondly, we fix the relative mutual inclination i_{tot} to zero and explore the entire uncertain parameter space by a grid of simulations with step sizes $\Delta a_B = 0.4$ AU and $\Delta e_B = 0.01$ (Supplementary Figure 2).

Lastly, we investigated the 2+1 configuration of HD 59686 composed of the host star A, companion star B, and planet b (Figure 4, right column and Supplementary Figure 3). Since the orbital orientation of the stellar binary and planet are less constrained, we opt to choose a reference frame in which $\Omega_B = \Omega_{Ab} = i_{Ab} = 0^\circ$ and set in each simulation the binary inclination to $i_B = i_{\text{tot}} = 0.0^\circ, 2.5^\circ, \dots, 180.0^\circ$. Component masses, eccentricities, binary semi-major axis, and planet orbital period are adopted from the observational mean values [42, Supplementary Table 1]. Assuming that we observe the system from a isotropically random direction, we divide the companion mass and planet mass by the sines of the line-of-sight inclinations, respectively, and calculate the planet semi-major axis from Eq. (2). The remaining angles are randomly sampled.

Sources of precession and its effects on the dynamics

In realistic systems, the planet TOI 4633c might be stabilised by relativistic and tidal effects which cause its orbit to precess quenching the perturbation from the stellar companion [e.g., 55]. These effects are not included in our simulations. However, we show below that they are expected to be less important than the precession in the vZLK



Supplementary Figure 1 Same as Figure 4 for different configurations of TOI 4633 (see description in the Methods).

Parameters	TOI 4633 [1]	HD 59686 [42]
<i>Outer orbit of the stars:</i>		
Host mass m_A [M_\odot]	1.10 ± 0.06	1.9 ± 0.2
Companion mass m_B [M_\odot]	1.05 ± 0.06	$0.5293^{+0.0011}_{-0.0009} \times (\sin i_B)^{-1}$
Age t_{age} [Gyr]	1.3 ± 0.3	1.73 ± 0.47
Host radius r_A [R_\odot]	1.05 ± 0.05	13.2 ± 0.3
Semi-major axis a_B [AU]	$48.6^{+4.4}_{-3.5}$	$13.56^{+0.18}_{-0.14}$
Orbital period T_B [yr]	231^{+32}_{-24}	$31.98^{+0.64}_{-0.47}$
Eccentricity e_B	0.91 ± 0.03	$0.729^{+0.004}_{-0.003}$
Argument of pericentre ω_B [deg]	110.5 ± 2.1	149.4 ± 0.2
Longitude of ascending node Ω_B [deg]	$123.5^{+3.3}_{-2.9}$	n/a
Inclination i_B [deg]	90.1 ± 0.4	n/a
<i>Orbit of the inner planet:</i>		
	TOI 4633b ¹	HD 59686b
Planet minimum mass $m_b \sin i_{Ab}$ [M_\oplus]	$106.8^{+13.0}_{-12.8}$	$2199.18^{+57.20}_{-76.27}$
Orbital period T_{Ab} [days]	34.15 ± 0.15	$299.36^{+0.26}_{-0.31}$
Eccentricity e_{Ab}	$0.096^{+0.102}_{-0.065}$	$0.05^{+0.03}_{-0.02}$
Argument of pericentre ω_{Ab} [deg]	$-43.9^{+104.8}_{-72.8}$	121^{+28}_{-24}
Longitude of ascending node Ω_{Ab} [deg]	n/a	n/a
Inclination i_{Ab} [deg]	≈ 90.0 (not transiting)	n/a
<i>Orbit of the outer planet:</i>		
	TOI 4633c	
Planet mass m_c [M_\oplus]	$47.8^{+27.6}_{-23.8}$	
Planet radius r_c [R_\oplus]	$3.2^{+0.20}_{-0.19}$	
Semi-major axis a_{Ac} [AU]	0.847 ± 0.061	
Critical semi-major axis ² a_{crit} [AU]	$0.47^{+0.35}_{-0.28}$	
Orbital period T_{Ac} [days]	$271.9445^{+0.0039}_{-0.0040}$	
Eccentricity e_{Ac}	$0.117^{+0.189}_{-0.085}$	
Argument of pericentre ω_{Ac} [deg]	-21^{+131}_{-108}	
Longitude of asc. node Ω_{Ac} [deg]	n/a	
Inclination i_{Ac} [deg]	$89.888^{+0.069}_{-0.064}$	

¹Observations do not tell whether the planet TOI 4633b is orbiting star TOI 4633A or B [1]. Nonetheless, we denote its parameters with subscripts “b” and “Ab” for the ease of reading.

² $a_{\text{crit}} = [(0.464 \pm 0.006) + (-0.380 \pm 0.010)\mu + (-0.631 \pm 0.034)e_B + (0.586 \pm 0.061)\mu e + (0.150 \pm 0.041)e_B^2 + (-0.198 \pm 0.074)\mu e_B^2] a_B$ where $\mu = m_B/(m_A + m_B)$ [2].

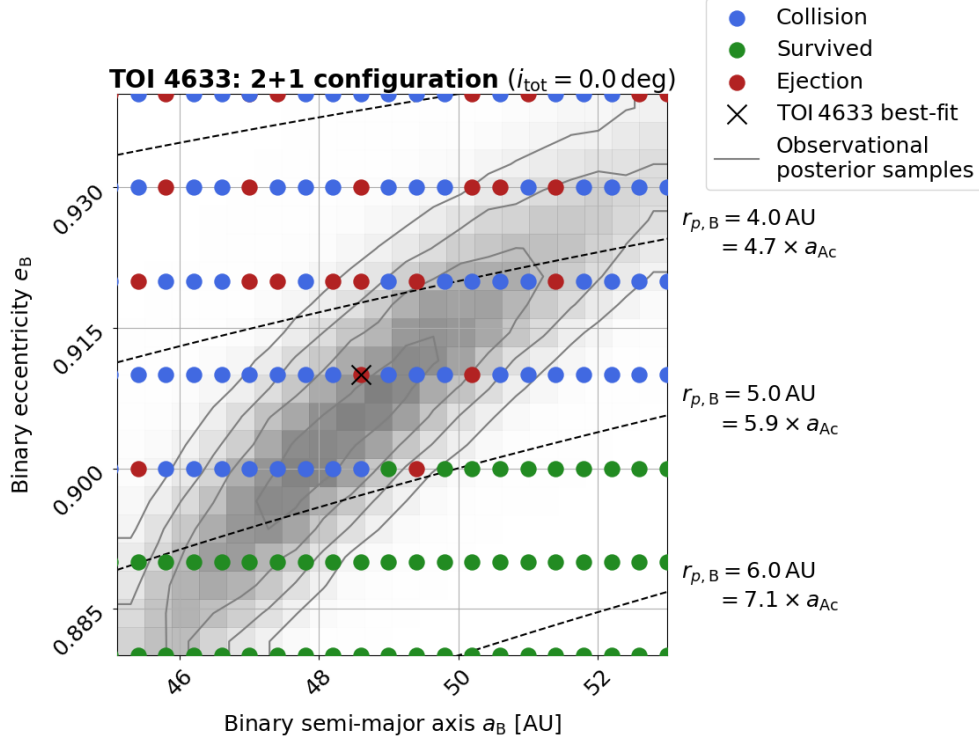
Supplementary Table 1 Orbital parameter values of the two planetary systems TOI 4633 and HD 59686 inferred by Eisner et al. [1] and Ortiz et al. [42], respectively. TOI 4633 harbours two known planets, HD 59686 just one.

dynamics and the precession arising from the presence of the inner planet TOI 4633b (in the 3+1 configuration) highlighting the robustness of our results.

Schwarzschild precession from general relativity

The relativistic Schwarzschild precession can be compared to the secular precession rate from the outer stellar companion. The dimensionless precession rate is given by ϵ_{GR} [56, 57]:

$$\epsilon_{\text{GR}} \equiv \left| \frac{\dot{\omega}_{\text{Ac,GR}}}{\dot{\omega}_{\text{Ac,vZLK}}} \right| = \frac{3m_{\text{bin}}}{m_{\text{out}}} \frac{a_B^3 (1 - e_B)^{3/2}}{a_{\text{Ac}}^3} \frac{Gm_{\text{bin}}}{a_{\text{Ac}} c^2}, \quad (3)$$

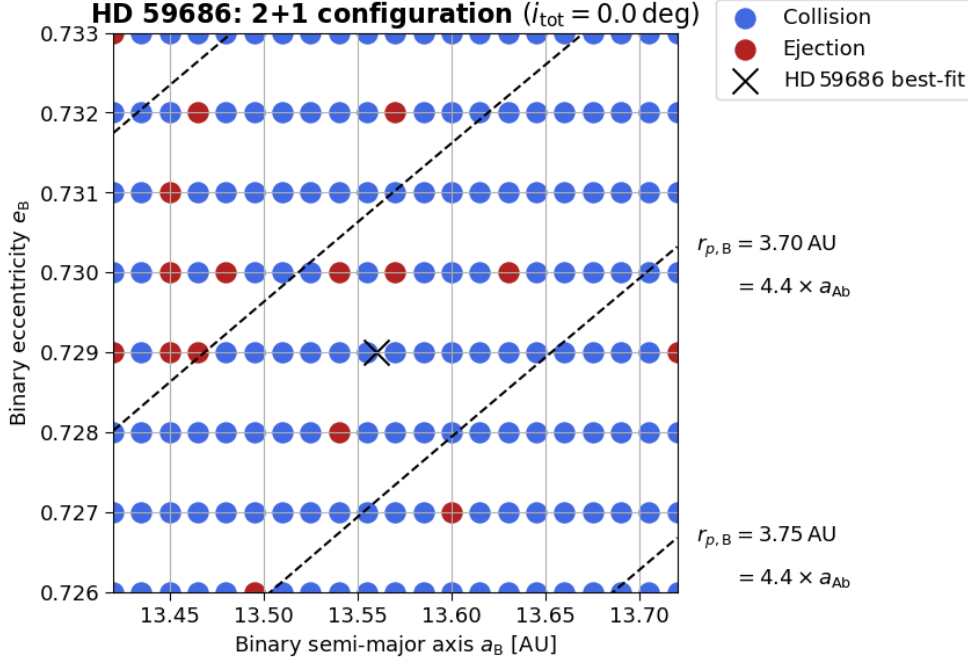


Supplementary Figure 2 Evolutionary outcomes within the observational one-sigma uncertainty of the binary semi-major axis $a_B = 48.6^{+4.4}_{-3.5}$ AU and orbital eccentricity $e_B = 0.91 \pm 0.03$. We consider our default 2+1 configuration and assume TOI4633c to be on a prograde orbit ($i_{\text{tot}} = 0.0^\circ$). As in Figure 4, green, blue, and red markers indicate the survival of the system, the collision of the planet with a star, and a planetary ejection. The black cross indicates the best observational fit to the orbital binary parameters of TOI4633AB at $a_B = 48.6$ AU and $e_B = 0.91$, while grey (0.5, 1, 1.5, 2)-sigma equivalent contours indicate the two-dimensional posterior distribution of a_B and e_B from the observational data of TOI4633 [1, see Fig. 7]. The boundaries of the plot match the observational one-sigma uncertainties of the marginal posterior distributions of a_B and e_B . Dashed contour lines show constant values for the binary periastron at $r_{p,B} = 3.0, 4.0, 5.0,$ and 6.0 AU.

where $m_{\text{bin}} = m_A + m_c$, $m_{\text{out}} = m_B$. For $\epsilon_{\text{GR}} \gg 1$ the effects from the stellar companion are negligible, while for $\epsilon_{\text{GR}} \ll 1$ the relativistic effect is small. Nevertheless, for small $\epsilon_{\text{GR}} \ll 1$ the maximal eccentricity is limited by $e_{\text{max}} = \sqrt{1 - 8\epsilon_{\text{GR}}^2/9}$, even for optimal mutual inclination. For the parameters of planet c we have $\epsilon_{\text{GR}} = 5 \times 10^{-4}$ and $1 - e_{\text{max}} \approx 10^{-6}$ which is insignificant. We conclude that the extra precession from general relativity does not affect the long-term dynamics of the TOI4633 system.

Precession from tidal bulges

Tidal interactions can raise equilibrium bulges on the planets and stars. This deviation from spherical symmetry will also lead to precession. The relative strength of the precession is parametrised by the apsidal motion constants $k_{1\star}$ and k_{1p} for the stars



Supplementary Figure 3 Same as Supplementary Figure 2 for HD 59686.

and planets respectively. Similarly, we can define the relative precession rate compared to the vZLK one [56, 57]

$$\epsilon_{\text{tide}} \equiv \left| \frac{\dot{\omega}_{\text{Ac,tide}}}{\dot{\omega}_{\text{Ac,vZLK}}} \right| = \frac{15m_{\text{bin}}a_{\text{B}}^3(1-e_{\text{B}})^{3/2}(k_{1\star}m_{\text{A}}^2R_{\text{A}}^5 + k_{1\text{p}}m_{\text{c}}^2R_{\text{Ac}}^5)}{a_{\text{Ac}}^8m_{\text{A}}m_{\text{c}}m_{\text{B}}} \quad (4)$$

where the two terms measure the tidal bulges raised on the star A and the planet c. The apsidal motion constants are $k_{1\star} = 0.014$, $k_{1\text{p}} = 0.1$ (e.g. [58]) and the radii are $r_{\text{A}} = 1.05 R_{\odot}$, $r_{\text{c}} = 0.05 R_{\odot}$. For the parameters of planet c, we have $\epsilon_{\text{tide}} \approx 2 \times 10^{-4}$. The maximal eccentricity can be solved numerically, yielding $e_{\text{max}} \approx 0.92$. Similarly, for planet b, tides are more important, yielding $\epsilon_{\text{tide}} \approx 4.16$ and $e_{\text{max}} \approx 0.43$, which could contribute to the stability on the inner planet. We conclude that tidal bulges may have greater importance than the Schwarzschild effect, but still could be safely ignored for the duration of the dynamical evolution of the outer planet.

Precession from inner mass quadrupole

The inner planet may also affect the orbit of planet c. In order to estimate this effect, we first define the “effective Laplace radius” [59] which measures the relative importance of the inner quadrupole moment relative to the outer quadrupole perturbation from

the binary companion:

$$r_L = \left(\frac{m_A m_b}{2m_B(m_A + m_b)} a_{Ab}^2 a_B^3 (1 - e_B^2)^{3/2} \right)^{1/5}. \quad (5)$$

For our case, we have $r_L \approx 0.615$ AU, which is slightly smaller than the planet *c*'s current location. The relative precession rate of planet *c* compared to the vZKL rate is $\epsilon_{\text{rot}} = 1.5(a_{Ac}/r_L)^{-5} \approx 0.3$. The maximal eccentricity can also be computed via (e.g. [60]) $e_{\text{max}} = 1 - 2\epsilon_{\text{rot}}^{2/3}/9 \approx 0.9$.

We conclude that the inner mass quadrupole from the inner planet *b* is the most important effect, but still, the maximal eccentricity can reach very high values of almost 0.9. We simulate four-body systems that capture this effect in Supplementary Figure 1 and find similar results when only retrograde planetary orbits are stable for 10^9 yr. Moreover, since lower eccentricity is required for a close encounter with the inner planet, more systems become unstable on average and the instability times are somewhat shorter for the prograde orbits.

Precession of the outer orbit due to planet *c*

Similarly, we can estimate the precession timescale for the binary stellar orbit as seen in Figure 3. The precession timescale is a product of the mass ratios between the planets and the stars and the square of the semi-latus rectum of the outer orbit to the planet's semi-major axis:

$$T_{\text{prec,B}} \approx T_B \times \frac{m_A + m_B}{m_{Ac}} \frac{a_B(1 - e_B^2)}{a_{Ac}^2} \approx 170 \text{ Myr}. \quad (6)$$

The timescale is consistent with the observed precession of a few degrees during the integration time reported in Figure 3.

Acknowledgements

This research has made use of data obtained from or tools provided by the portal exoplanet.eu of The Extrasolar Planets Encyclopaedia [5]. J.S., S.J., and S.E.d.M. acknowledge funding from the Netherlands Organisation for Scientific Research (NWO), as part of the Vidi research program BinWaves (project No. 639.042.728, PI: de Mink). C.J. acknowledges funding from the Royal Society through the Newton International Fellowship funding scheme (project No. NIF\R1\242552). Computations were performed on the HPC system Raven at the Max Planck Computing and Data Facility.

Author contributions

J.S. conceived the study, performed the numerical and analytical computations, and wrote the manuscript. E.G. contributed to the numerical computations and analytical calculations. C.J. and N.L.E. provided observational expertise of TOI 4633. H.B.P. contributed to the stability analysis and relation of stability and post-snow-line planet

formation. All authors contributed to the interpretation of the results and reviewed and edited the manuscript.

Declarations

The authors declare no competing interests.

References

- [1] Eisner, N.L., Grunblatt, S.K., Barragán, O., Faridani, T.H., Lintott, C., Aigrain, S., Johnston, C., Mason, I.R., Stassun, K.G., Bedell, M., Boyle, A.W., Ciardi, D.R., Clark, C.A., Hebrard, G., Hogg, D.W., Howell, S.B., Klein, B., Llama, J., Winn, J.N., Zhao, L.L., Murphy, J.M.A., Beard, C., Brinkman, C.L., Chontos, A., Cortes-Zuleta, P., Delfosse, X., Giacalone, S., Gilbert, E.A., Heidari, N., Holcomb, R., Jenkins, J.M., Kiefer, F., Lubin, J., Martioli, E., Polanski, A.S., Saunders, N., Seager, S., Shporer, A., Tyler, D., Van Zandt, J., Alhassan, S., Amratlal, D.J., Antonel, L.I., Bentzen, S.L.S., Bosch, M.K.D., Bundy, D., Chitsiga, I., Delaunay, J.F., Doisy, X., Ferstenou, R., Fynø, M., Geary, J.M., Haynaly, G., Hermes, P., Hutten, M., Lee, S., Metcalfe, P., Pennell, G.J., Puzskarska, J., Schäfer, T., Stiller, L., Tanner, C., Tarr, A., Wilkinson, A.: Planet Hunters TESS. V. A Planetary System Around a Binary Star, Including a Mini-Neptune in the Habitable Zone. *Astron. J.* **167**(5), 241 (2024) <https://doi.org/10.3847/1538-3881/ad1d5c> [arXiv:2404.18997](https://arxiv.org/abs/2404.18997) [astro-ph.EP]
- [2] Holman, M.J., Wiegert, P.A.: Long-Term Stability of Planets in Binary Systems. *Astron. J.* **117**(1), 621–628 (1999) <https://doi.org/10.1086/300695> [arXiv:astro-ph/9809315](https://arxiv.org/abs/astro-ph/9809315) [astro-ph]
- [3] Hayashi, C.: Structure of the Solar Nebula, Growth and Decay of Magnetic Fields and Effects of Magnetic and Turbulent Viscosities on the Nebula. *Progress of Theoretical Physics Supplement* **70**, 35–53 (1981) <https://doi.org/10.1143/PTPS.70.35>
- [4] Ida, S., Lin, D.N.C.: Toward a Deterministic Model of Planetary Formation. III. Mass Distribution of Short-Period Planets around Stars of Various Masses. *Astrophys. J.* **626**(2), 1045–1060 (2005) <https://doi.org/10.1086/429953> [arXiv:astro-ph/0502566](https://arxiv.org/abs/astro-ph/0502566) [astro-ph]
- [5] Kral, Q.: The Encyclopaedia of Exoplanetary Systems. <https://exoplanet.eu/home/>
- [6] Quarles, B., Li, G., Kostov, V., Haghighipour, N.: Orbital Stability of Circumstellar Planets in Binary Systems. *Astron. J.* **159**(3), 80 (2020) <https://doi.org/10.3847/1538-3881/ab64fa> [arXiv:1912.11019](https://arxiv.org/abs/1912.11019) [astro-ph.EP]
- [7] Lee, M.H., Wong, K.H., Cheng, H.W., Trifonov, T., Reffert, S., Quirrenbach, A.: Dynamics of Circumstellar Planets in Binary Star Systems. In: Lemaître, A.,

- Libert, A.-S. (eds.) IAU Symposium. IAU Symposium, vol. 382, pp. 12–19 (2024). <https://doi.org/10.1017/S1743921323004787>
- [8] Pilat-Lohinger, E., Dvorak, R.: Stability of S-type Orbits in Binaries. *Celestial Mechanics and Dynamical Astronomy* **82**(2), 143–153 (2002) <https://doi.org/10.1023/A:1014586308539>
- [9] David, E.-M., Quintana, E.V., Fatuzzo, M., Adams, F.C.: Dynamical Stability of Earth-like Planetary Orbits in Binary Systems. *Publ. Astron. Soc. Pac.* **115**(809), 825–836 (2003) <https://doi.org/10.1086/376395> [arXiv:astro-ph/0304561](https://arxiv.org/abs/astro-ph/0304561) [astro-ph]
- [10] Pilat-Lohinger, E., Funk, B., Dvorak, R.: Stability limits in double stars. A study of inclined planetary orbits. *Astron. Astrophys.* **400**, 1085–1094 (2003) <https://doi.org/10.1051/0004-6361:20021811>
- [11] Barnes, R., Quinn, T.: The (In)stability of Planetary Systems. *Astrophys. J.* **611**(1), 494–516 (2004) <https://doi.org/10.1086/421321> [arXiv:astro-ph/0401171](https://arxiv.org/abs/astro-ph/0401171) [astro-ph]
- [12] Musielak, Z.E., Cuntz, M., Marshall, E.A., Stuit, T.D.: Stability of planetary orbits in binary systems. *Astron. Astrophys.* **434**(1), 355–364 (2005) <https://doi.org/10.1051/0004-6361:20040238>
- [13] Fatuzzo, M., Adams, F.C., Gauvin, R., Proszkow, E.M.: A Statistical Stability Analysis of Earth-like Planetary Orbits in Binary Systems. *Publ. Astron. Soc. Pac.* **118**(849), 1510–1527 (2006) <https://doi.org/10.1086/508999> [arXiv:astro-ph/0609305](https://arxiv.org/abs/astro-ph/0609305) [astro-ph]
- [14] Marzari, F., Barbieri, M.: Planets in binary systems: is the present configuration indicative of the formation process? *Astron. Astrophys.* **467**(1), 347–351 (2007) <https://doi.org/10.1051/0004-6361:20077102> [arXiv:astro-ph/0702342](https://arxiv.org/abs/astro-ph/0702342) [astro-ph]
- [15] Quarles, B., Lissauer, J.J.: Long-term Stability of Planets in the α Centauri System. *Astron. J.* **151**(5), 111 (2016) <https://doi.org/10.3847/0004-6256/151/5/111> [arXiv:1604.04917](https://arxiv.org/abs/1604.04917) [astro-ph.EP]
- [16] Trifonov, T., Lee, M.H., Reffert, S., Quirrenbach, A.: Dynamical Analysis of the Circumprimary Planet in the Eccentric Binary System HD 59686. *Astron. J.* **155**(4), 174 (2018) <https://doi.org/10.3847/1538-3881/aab439> [arXiv:1803.01434](https://arxiv.org/abs/1803.01434) [astro-ph.EP]
- [17] Quarles, B., Gautham Bhaskar, H., Li, G.: Main-sequence systems: orbital stability in stellar binaries. *arXiv e-prints*, 2407–13901 (2024) <https://doi.org/10.48550/arXiv.2407.13901> [arXiv:2407.13901](https://arxiv.org/abs/2407.13901) [astro-ph.EP]
- [18] Rein, H., Liu, S.-F.: REBOUND: an open-source multi-purpose N-body code

- for collisional dynamics. *Astron. Astrophys.* **537**, 128 (2012) <https://doi.org/10.1051/0004-6361/201118085> arXiv:1110.4876 [astro-ph.EP]
- [19] Miret-Roig, N., Bouy, H., Raymond, S.N., Tamura, M., Bertin, E., Barrado, D., Olivares, J., Galli, P.A.B., Cuillandre, J.-C., Sarro, L.M., Berihuete, A., Huélamo, N.: A rich population of free-floating planets in the Upper Scorpius young stellar association. *Nature Astronomy* **6**, 89–97 (2022) <https://doi.org/10.1038/s41550-021-01513-x> arXiv:2112.11999 [astro-ph.EP]
- [20] Kratter, K.M., Perets, H.B.: Star hoppers: Planet instability and capture in evolving binary systems. *The Astrophysical Journal* **753**(1), 91 (2012) <https://doi.org/10.1088/0004-637X/753/1/91>
- [21] Harrington, R.S.: Stability Criteria for Triple Stars. *Celestial Mechanics* **6**(3), 322–327 (1972) <https://doi.org/10.1007/BF01231475>
- [22] Innanen, K.A.: The Coriolis asymmetry in the classical restricted 3-body problem and the Jacobian integral. *Astron. J.* **85**, 81–85 (1980) <https://doi.org/10.1086/112642>
- [23] Zeipel, H.V.: Sur l’application des séries de m. lindstedt à l’étude du mouvement des comètes périodiques. *Astronomische Nachrichten* **183**(22-24), 345–418 (1909) <https://doi.org/10.1002/asna.19091832202> <https://onlinelibrary.wiley.com/doi/pdf/10.1002/asna.19091832202>
- [24] Kozai, Y.: Secular perturbations of asteroids with high inclination and eccentricity. *AJ* **67**, 591–598 (1962) <https://doi.org/10.1086/108790>
- [25] Lidov, M.L.: The evolution of orbits of artificial satellites of planets under the action of gravitational perturbations of external bodies. *Planetary and Space Science* **9**(10), 719–759 (1962) [https://doi.org/10.1016/0032-0633\(62\)90129-0](https://doi.org/10.1016/0032-0633(62)90129-0)
- [26] Perets, H.B., Kratter, K.M.: The Triple Evolution Dynamical Instability: Stellar Collisions in the Field and the Formation of Exotic Binaries. *Astrophys. J.* **760**(2), 99 (2012) <https://doi.org/10.1088/0004-637X/760/2/99> arXiv:1203.2914 [astro-ph.SR]
- [27] Grishin, E., Perets, H.B., Zenati, Y., Michaely, E.: Generalized Hill-stability criteria for hierarchical three-body systems at arbitrary inclinations. *Mon. Not. R. Astron. Soc.* **466**(1), 276–285 (2017) <https://doi.org/10.1093/mnras/stw3096> arXiv:1609.05912 [astro-ph.EP]
- [28] Tanaka, H., Takeuchi, T., Ward, W.R.: Three-Dimensional Interaction between a Planet and an Isothermal Gaseous Disk. I. Corotation and Lindblad Torques and Planet Migration. *Astrophys. J.* **565**(2), 1257–1274 (2002) <https://doi.org/10.1086/324713>

- [29] Mizuno, H.: Formation of the Giant Planets. *Progress of Theoretical Physics* **64**(2), 544–557 (1980) <https://doi.org/10.1143/PTP.64.544>
- [30] Pollack, J.B.: Origin and History of the Outer Planets: Theoretical Models and Observations L Constraints. *Annu. Rev. Astron. Astrophys.* **22**, 389–424 (1984) <https://doi.org/10.1146/annurev.aa.22.090184.002133>
- [31] Lissauer, J.J.: Planet formation. *Annu. Rev. Astron. Astrophys.* **31**, 129–174 (1993) <https://doi.org/10.1146/annurev.aa.31.090193.001021>
- [32] Kraus, A.L., Ireland, M.J., Hillenbrand, L.A., Martinache, F.: The Role of Multiplicity in Disk Evolution and Planet Formation. *Astrophys. J.* **745**(1), 19 (2012) <https://doi.org/10.1088/0004-637X/745/1/19> arXiv:1109.4141 [astro-ph.EP]
- [33] Kraus, A.L., Ireland, M.J., Huber, D., Mann, A.W., Dupuy, T.J.: The Impact of Stellar Multiplicity on Planetary Systems. I. The Ruinous Influence of Close Binary Companions. *Astron. J.* **152**(1), 8 (2016) <https://doi.org/10.3847/0004-6256/152/1/8> arXiv:1604.05744 [astro-ph.EP]
- [34] Xie, J.-W., Zhou, J.-L., Ge, J.: Planetesimal Accretion in Binary Systems: Could Planets Form Around α Centauri B? *Astrophys. J.* **708**(2), 1566–1578 (2010) <https://doi.org/10.1088/0004-637X/708/2/1566> arXiv:1001.2614 [astro-ph.EP]
- [35] Rafikov, R.R., Silsbee, K.: Planet Formation in Stellar Binaries. II. Overcoming the Fragmentation Barrier in α Centauri and γ Cephei-like Systems. *Astrophys. J.* **798**(2), 70 (2015) <https://doi.org/10.1088/0004-637X/798/2/70> arXiv:1408.4819 [astro-ph.EP]
- [36] Generozov, A., Offner, S.S.R., Kratter, K.M., Perets, H.B., Guszejnov, D., Grudić, M.Y.: Stellar Binaries are Bound from Birth. *Nature*, submitted (2025)
- [37] Heggie, D.C.: Binary evolution in stellar dynamics. *Mon. Not. R. Astron. Soc.* **173**, 729–787 (1975) <https://doi.org/10.1093/mnras/173.3.729>
- [38] Ostriker, E.C.: Capture and Induced Disk Accretion in Young Star Encounters. *Astrophys. J.* **424**, 292 (1994) <https://doi.org/10.1086/173890>
- [39] Mardling, R.A., Aarseth, S.J.: Tidal interactions in star cluster simulations. *Mon. Not. R. Astron. Soc.* **321**(3), 398–420 (2001) <https://doi.org/10.1046/j.1365-8711.2001.03974.x>
- [40] Naoz, S., Farr, W.M., Lithwick, Y., Rasio, F.A., Teyssandier, J.: Hot Jupiters from secular planet-planet interactions. *Nature* **473**(7346), 187–189 (2011) <https://doi.org/10.1038/nature10076> arXiv:1011.2501 [astro-ph.EP]
- [41] Gong, Y.-X., Ji, J.: Formation of S-type planets in close binaries: scattering-induced tidal capture of circumbinary planets. *Mon. Not. R.*

- Astron. Soc. **478**(4), 4565–4574 (2018) <https://doi.org/10.1093/mnras/sty1300> [arXiv:1805.05868](https://arxiv.org/abs/1805.05868) [astro-ph.EP]
- [42] Ortiz, M., Reffert, S., Trifonov, T., Quirrenbach, A., Mitchell, D.S., Nowak, G., Buenzli, E., Zimmerman, N., Bonnefoy, M., Skemer, A., Defrère, D., Lee, M.H., Fischer, D.A., Hinz, P.M.: Precise radial velocities of giant stars. IX. HD 59686 Ab: a massive circumstellar planet orbiting a giant star in a 13.6 au eccentric binary system. *Astron. Astrophys.* **595**, 55 (2016) <https://doi.org/10.1051/0004-6361/201628791> [arXiv:1608.00963](https://arxiv.org/abs/1608.00963) [astro-ph.EP]
- [43] Perets, H.B.: Second generation planets. arXiv e-prints, 1001–0581 (2010) <https://doi.org/10.48550/arXiv.1001.0581> [arXiv:1001.0581](https://arxiv.org/abs/1001.0581) [astro-ph.EP]
- [44] Tutukov, A.V., Fedorova, A.V.: Formation of planets during the evolution of single and binary stars. *Astronomy Reports* **56**(4), 305–314 (2012) <https://doi.org/10.1134/S1063772912040075>
- [45] European Space Agency (ESA): Plato definition study report (red book). ESA-SCI 2017/1, European Space Agency (ESA) (April 2017). <https://sci.esa.int/s/8rPypEw>
- [46] Offner, S.S.R., Moe, M., Kratter, K.M., Sadavoy, S.I., Jensen, E.L.N., Tobin, J.J.: The Origin and Evolution of Multiple Star Systems. In: Inutsuka, S., Aikawa, Y., Muto, T., Tomida, K., Tamura, M. (eds.) *Protostars and Planets VII*. Astronomical Society of the Pacific Conference Series, vol. 534, p. 275 (2023). <https://doi.org/10.48550/arXiv.2203.10066>
- [47] Rossiter, R.A.: On the detection of an effect of rotation during eclipse in the velocity of the brighter component of beta Lyrae, and on the constancy of velocity of this system. *Astrophys. J.* **60**, 15–21 (1924) <https://doi.org/10.1086/142825>
- [48] McLaughlin, D.B.: Some results of a spectrographic study of the Algol system. *Astrophys. J.* **60**, 22–31 (1924) <https://doi.org/10.1086/142826>
- [49] Albrecht, S.H., Dawson, R.I., Winn, J.N.: Stellar Obliquities in Exoplanetary Systems. *Publ. Astron. Soc. Pac.* **134**(1038), 082001 (2022) <https://doi.org/10.1088/1538-3873/ac6c09> [arXiv:2203.05460](https://arxiv.org/abs/2203.05460) [astro-ph.EP]
- [50] Gragg, W.B.: On Extrapolation Algorithms for Ordinary Initial Value Problems. *SIAM Journal on Numerical Analysis* **2**, 384–403 (1965) <https://doi.org/10.1137/0702030>
- [51] Bulirsch, R., Stoer, J.: Numerical treatment of ordinary differential equations by extrapolation methods. *Numerische Mathematik* **8**(1), 1–13 (1966)
- [52] Everhart, E.: An efficient integrator that uses Gauss-Radau spacings. In: Carusi, A., Valsecchi, G.B. (eds.) *IAU Colloq. 83: Dynamics of Comets: Their Origin*

and Evolution. Astrophysics and Space Science Library, vol. 115, p. 185 (1985).
https://doi.org/10.1007/978-94-009-5400-7_17

- [53] Rein, H., Spiegel, D.S.: IAS15: a fast, adaptive, high-order integrator for gravitational dynamics, accurate to machine precision over a billion orbits. *Mon. Not. R. Astron. Soc.* **446**(2), 1424–1437 (2015) <https://doi.org/10.1093/mnras/stu2164> [arXiv:1409.4779](https://arxiv.org/abs/1409.4779) [astro-ph.EP]
- [54] Müller, S., Baron, J., Helled, R., Bouchy, F., Parc, L.: The mass-radius relation of exoplanets revisited. *Astron. Astrophys.* **686**, 296 (2024) <https://doi.org/10.1051/0004-6361/202348690> [arXiv:2311.12593](https://arxiv.org/abs/2311.12593) [astro-ph.EP]
- [55] Liu, B., Muñoz, D.J., Lai, D.: Suppression of extreme orbital evolution in triple systems with short-range forces. *Mon. Not. R. Astron. Soc.* **447**(1), 747–764 (2015) <https://doi.org/10.1093/mnras/stu2396> [arXiv:1409.6717](https://arxiv.org/abs/1409.6717) [astro-ph.EP]
- [56] Liu, B., Muñoz, D.J., Lai, D.: Suppression of extreme orbital evolution in triple systems with short-range forces. *Mon. Not. R. Astron. Soc.* **447**(1), 747–764 (2015) <https://doi.org/10.1093/mnras/stu2396> [arXiv:1409.6717](https://arxiv.org/abs/1409.6717) [astro-ph.EP]
- [57] Mangipudi, A., Grishin, E., Trani, A.A., Mandel, I.: Extreme Eccentricities of Triple Systems: Analytic Results. *Astrophys. J.* **934**(1), 44 (2022) <https://doi.org/10.3847/1538-4357/ac7958> [arXiv:2205.08703](https://arxiv.org/abs/2205.08703) [astro-ph.EP]
- [58] Grishin, E., Perets, H.B.: Chaotic dynamics of wide triples induced by galactic tides: a novel channel for producing compact binaries, mergers, and collisions. *Mon. Not. R. Astron. Soc.* **512**(4), 4993–5009 (2022) <https://doi.org/10.1093/mnras/stac706> [arXiv:2112.11475](https://arxiv.org/abs/2112.11475) [astro-ph.SR]
- [59] Grishin, E., Lai, D., Perets, H.B.: Chaotic quadruple secular evolution and the production of misaligned exomoons and Warm Jupiters in stellar multiples. *Mon. Not. R. Astron. Soc.* **474**(3), 3547–3556 (2018) <https://doi.org/10.1093/mnras/stx3005> [arXiv:1710.05920](https://arxiv.org/abs/1710.05920) [astro-ph.EP]
- [60] Grishin, E., Malamud, U., Perets, H.B., Wandel, O., Schäfer, C.M.: The wide-binary origin of (2014) MU₆₉-like Kuiper belt contact binaries. *Nature* **580**(7804), 463–466 (2020) <https://doi.org/10.1038/s41586-020-2194-z> [arXiv:2003.01720](https://arxiv.org/abs/2003.01720) [astro-ph.EP]